



Available online at www.sciencedirect.com

ScienceDirect

journal homepage: www.e-jds.com



Original Article

Evaluation of morphological, histological, and immune-related cellular changes in ligature-induced experimental periodontitis in mice

Shiyi Li ^{a†}, Wenmin Zeng ^{a†}, Guojing Liu ^a, Jing Zang ^b,
Xiaoqian Yu ^{a*}

^a Department of Periodontology, Peking University School and Hospital of Stomatology, Beijing, China

^b Department of Periodontology, Peking University Third Hospital, Beijing, China

Received 22 December 2022; Final revision received 2 January 2023

Available online 12 January 2023

KEYWORDS

Experimental periodontitis;
Immune cell;
Inflammation;
Mice;
Periodontal tissue

Abstract *Background/purpose:* The ligature-induced periodontitis model is an effective approach to induce inflammation and bone loss similar to that of human periodontitis. Previous clinical and *in vitro* studies have shown the involvement of lymphocytes in periodontitis, while, the local and systemic profile of immune cells associated with periodontitis in the ligature-induced periodontitis model in mice remains unclear.

Materials and methods: Experimental periodontitis was constructed in mice by ligating around the maxillary second molars for 14 and 28 days, respectively. Alveolar bone loss was assessed by micro-computed tomography (micro-CT). Hematoxylin and eosin (H&E) and tartrate-resistant acid phosphatase (TRAP) staining were used to evaluate the histological changes in the periodontal tissues. B and T cells in the cervical lymph nodes, spleen, and peripheral blood were analyzed by flow cytometry.

Results: The 14-day ligation effectively induced significant periodontal inflammation and alveolar bone loss in C57BL/6J mice, which were progressive and maintained for a relatively long-term period until day 28. In addition, CD3⁺ T cells and CD19⁺ B cells were the dominant population in both health and disease, and the B cell population within the cervical lymph nodes (LN) increased significantly under periodontitis condition, while, no significant differences of the T and B cell population among the spleen and peripheral blood were observed.

* Corresponding author. Department of Periodontology, Peking University School and Hospital of Stomatology, No.22, Zhongguancun South Avenue, Haidian District, Beijing, 100081, China.

E-mail address: y_pk@163.com (X. Yu).

† The two authors contributed equally to this work.

Conclusion: The ligature-induced periodontitis mice model was established to perform a longitudinal assessment of changes in periodontal tissues morphologically and histologically, meanwhile, explore the local and systemic changes of the predominant immune-associated cells.

© 2023 Association for Dental Sciences of the Republic of China. Publishing services by Elsevier B.V. This is an open access article under the CC BY-NC-ND license (<http://creativecommons.org/licenses/by-nc-nd/4.0/>).

Introduction

Periodontal disease is a chronic inflammatory disease characterized by inflammatory infiltration and progressive alveolar bone loss.¹ As one of the most prevalent oral diseases worldwide, periodontitis not only leads to teeth loss, but may also increase the incidence of a variety of systemic disorders.²

It is known that pathogenic bacteria play an initiating role and that the subsequent recruitment of immune cells and the release of cytokines, growth factors, and signaling molecules determine the progression and severity of periodontitis.^{3,4} Numerous animal models firmly support the association of T and B cells with periodontal bone resorption.⁵ An *in-vitro* study using the gingival tissues of chronic periodontitis patients reported that T cells were the predominant infiltrating cell subset and that activated T and B cells were the cellular source of receptor activator of nuclear factor κ B ligand (RANKL) for bone resorption.⁶ Additionally, Dutzan et al. evaluated the characterization of the human immune cell subsets at the gingival barrier, revealed that CD3⁺ T cells remained the dominant population in both health and disease, and the total number of T cells increased with 10-fold in disease; while, B cell population was almost undetectable in health but become evident in periodontitis.⁷

The ligature-induced periodontitis model has been considered as an effective approach to induce inflammation and bone loss similar to human periodontitis and an effective method for the exploration of molecular mechanism.⁸ Even though animal models have limitations, they are often superior in addressing mechanistic questions and serve as an essential link between hypotheses and human patients.⁹ To date, there are a series of *in vitro* or clinical studies involving the changes of lymphocytes in periodontitis.¹⁰ However, studies using the ligature model have mainly focused on gingival inflammation and alveolar bone loss, the profiles of immune cells associated with the pathogenesis and progression of periodontitis has not been reported in detail.

Therefore, in the present study, we established a ligature-induced periodontitis model in mice to evaluate longitudinal variation in periodontal tissues in terms of morphology and histology, meanwhile, explore the local and systemic changes of the predominant immune cells associated with periodontitis.

Materials and methods

Animals

Male C57BL/6J mice (6-week-old male, weighing 20–25 g) were used for this study. All experimental procedures were

approved by the Animal Welfare and Biomedical Ethics Committee of Peking University (LA201406) and conducted in accordance with the ARRIVE guidelines.¹¹

Experimental procedures

All animals were randomly allocated to three groups with eight mice in each group: non-ligation (C), 14-day ligation (L14), and 28-day ligation (L28), respectively. Mouse model of experimental periodontitis was constructed using the classic silk thread ligation method.¹² Briefly, mice were anesthetized with sodium pentobarbital (6 mg/100 g, intraperitoneal injection), 6-0 silk ligatures were tied around the maxillary second molars. The ligatures were checked every 2 days and were replaced immediately if not intact. At the end of the experiment, peripheral blood samples were collected under general anesthesia by heart puncture.¹³ Subsequently, mice were sacrificed and the spleens and cervical lymph nodes (LN) were harvested, then the bilateral maxillae were dissected.

Micro-computed tomography (micro-CT) analysis

The left maxillae were fixed in 4% neutral paraformaldehyde (PFA) for 24 h and stored in 70% ethanol at 4 °C until analysis. The key parameters of the micro-CT scanner (Siemens Medical Solutions USA, Inc., Malvern, PA, USA) were as follows: source voltage of 60 kV, current of 220 μ A, and resolution of 8.89 μ m. The three-dimensional (3D) images were measured by the Inveon Research Workshop software (Siemens Medical Solutions USA, Inc.).

Linear measurement: The height of alveolar bone loss was measured as the distance from the cemento-enamel junction (CEJ) to the alveolar bone crest (ABC). The buccal groove, palatal groove, mesio-buccal, disto-buccal, mesio-palatal, and disto-palatal sites of the maxillary second molars were chosen as the measurement sites.

Volumetric measurement: The amount of circumferential bone loss around the maxillary second molars was assessed following the protocol described previously.¹⁴ Briefly, contours were drawn beginning below the roof of the furcation and moving in the apical direction until the first appearance of the alveolar bone crest. The most distal root of the first molar and the most mesial root of the third molar were used as borders. All contours were drawn at regular intervals (every five data planes).

Histological analysis

The right maxillae were fixed in 4% neutral PFA for 24 h and decalcified in 10% ethylenediaminetetraacetic acid (pH 7.4) at 37 °C for four weeks. Specimens were embedded in

paraffin, 5 μm -thick sections were cut along the long axis of the molars in the buccal-lingual plane.

Hematoxylin and eosin (H&E) staining

Sections were deparaffinized, hydrated and stained with H&E (Solarbio, Beijing, China) to evaluate the extent of inflammatory infiltration and the other histopathological changes of periodontal tissues. Images were captured on a light microscope (Olympus, Tokyo, Japan).

Tartrate-resistant acid phosphatase (TRAP) staining

Sections were stained using TRAP immunohistochemical staining kits (Sigma-Aldrich, St Louis, MO, USA) in accordance with the manufacturer's procedure. After the sections were counterstained with hematoxylin, images were captured on a light microscope (Olympus). Osteoclasts were counted as TRAP⁺ cell with three or more nuclei along the alveolar bone surface, and results are presented as the number of TRAP⁺ cell per square millimeter.

Flow cytometric analysis

Peripheral blood mononuclear cells (PBMC) were purified with Mouse Lymphocyte Separation Medium (Solarbio), counted, and re-suspended in Roswell Park Memorial Institute (RPMI) 1640.

Spleen and cervical LN cells were collected by mashing the samples through a 70- μm cell strainer using the thumb-piece of a plunger removed from a 1-mL syringe. Red blood cells were lysed with 3 mL 1 \times Red Blood Cell Lysis Buffer (Biolegend, San Diego, CA, USA). Cells were filtered through another 70- μm cell strainer, counted, and re-suspended in RPMI1640.

For flow cytometry, 1 $\times 10^6$ cells from each sample were stained with combinations of fluorescence-conjugated

monoclonal antibodies, including CD3-APC/Cyanine7 (APC-Cy7), CD4-PerCP/Cyanine5.5 (PerCP-Cy5.5), CD8-FITC, CD19-APC. All the antibodies were from Biolegend. Samples were subjected to flow cytometry analysis using a Beckman Coulter Gallios flow cytometer (Beckman Coulter, Inc., Brea, CA, USA) and Flowjo software (Tree Star, Inc., San Carlos, CA, USA).

Statistical analysis

Data are presented as the mean \pm standard deviation (SD) and analyzed using SPSS 19.0 software. The normality of the data distribution was established using the Kolmogorov–Smirnov test, a one-way analysis of variance (ANOVA) or independent two-tailed Student t tests were used to evaluate differences. $P < 0.05$ was considered statistically significant.

Results

Alveolar bone loss

To analyze and compare the alveolar bone loss in the different groups, micro-CT analysis was performed. Linear bone loss was calculated as the sum of the CEJ–ABC distance at the six-sites (Fig. 1a and c). The distance of CEJ–ABC increased significantly after 14-day ligation (1.72 ± 0.10 mm vs. 0.89 ± 0.04 mm, $P < 0.001$), a small rise was observed in the group of 28-day ligation when compared with the group of 14-day ligation (1.90 ± 0.09 mm vs. 1.72 ± 0.10 mm, $P < 0.05$). Undoubtedly, the distance of CEJ–ABC reached the maximum after 28-day ligation (1.90 ± 0.09 mm vs. 0.89 ± 0.04 mm, $P < 0.001$).

The volumetric measurement showed a similar trend (Fig. 1b and d). Severe alveolar bone loss was induced two weeks after ligation (0.18 ± 0.01 mm³ vs. 0.05 ± 0.01 mm³,

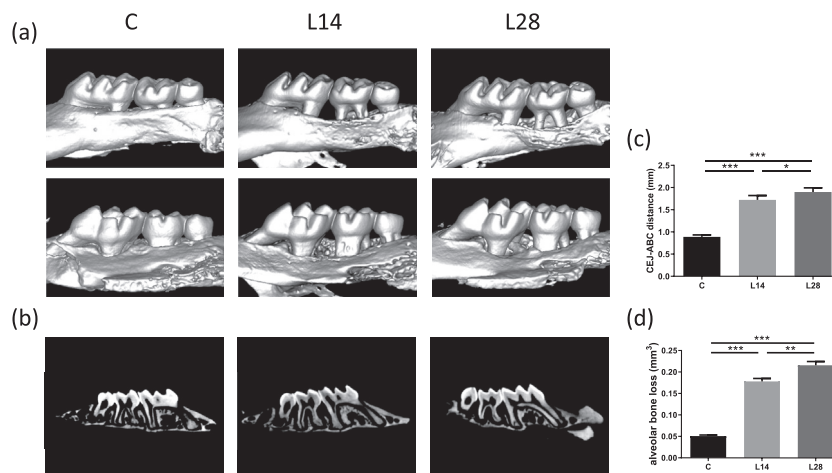


Fig. 1 Alveolar bone loss induced by ligation was assessed by micro-computed tomography. a) Representative three-dimensional views of the maxillae in the different groups. The upper panel shows the buccal surface, while the lower panel shows the palatal surface. b) The distances between the cemento-enamel junction and the alveolar bone crest of the maxillary second molars were measured and shown as mean \pm standard deviation. c) Representative images of maxilla in the sagittal plane. d) The volumes of the circumferential bone loss were shown as mean \pm standard deviation. The groups' names are abbreviated as follows: the control group (C), 14-day ligation group (L14), and 28-day ligation group (L28). * $P < 0.05$, ** $P < 0.01$, *** $P < 0.001$.

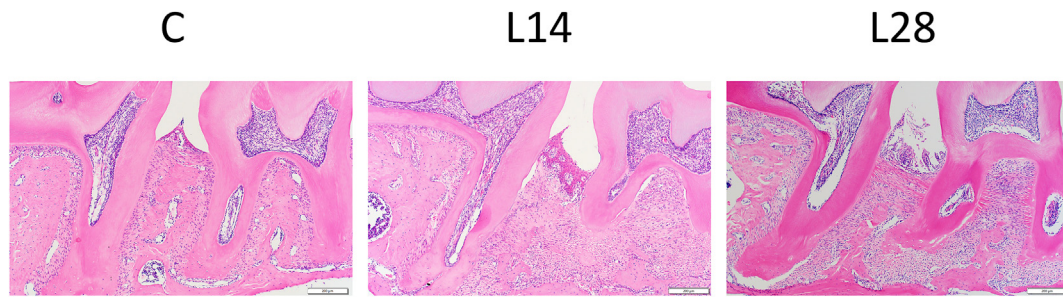


Fig. 2 Hematoxylin and eosin staining showed the extent of inflammatory infiltration and the other histopathological changes of periodontal tissues between the maxillary first molars and the maxillary second molars in the different groups. The groups' names are abbreviated as follows: the control group (C), 14-day ligation group (L14), and 28-day ligation group (L28). Scale bars: 200 μm .

$P < 0.001$), and the amount of circumferential bone loss further increased with the extension of ligation time until day 28 ($0.22 \pm 0.01 \text{ mm}^3$ vs. $0.18 \pm 0.01 \text{ mm}^3$, $P < 0.01$), resulting in a peak after 28-day ligation ($0.22 \pm 0.01 \text{ mm}^3$ vs. $0.05 \pm 0.01 \text{ mm}^3$, $P < 0.001$).

Histological observations

Inflammatory cell infiltration

H&E staining was performed to assess inflammatory cell infiltration and morphologic changes of the periodontium (Fig. 2). The control group showed the normal tissue structure. A triangular shape of the interproximal gingiva and a thick alveolar bone were observed. In addition, the junctional epithelium was attached along the root surface without the exposure of the CEJ.

The 14-day ligation caused significant hyperplasia of the epithelial nail process with the infiltration of a large number of inflammatory cells in the lamina propria. Evident bone resorption occurred at the adjacent region between the molars and the furcation area of the molars, also, attachment loss (AL) was observed.

The continuity of gingival epithelium was significantly destroyed on day 28. Epithelial ulceration, numerous inflammatory cell infiltration, severe bone loss, and AL were identified.

TRAP⁺ cell detection

TRAP staining was used to estimate the number of osteoclasts (Fig. 3). In the control group, the surface of the

alveolar bone crest was smooth and few TRAP⁺ cells were present. Two weeks after ligation, irregular alveolar bone surface was observed, and the number of TRAP⁺ cells was markedly increased ($P < 0.001$). In the group of 28-day ligation, the alveolar bone surface was more irregular with obvious bone resorption of lacunae, but the number of TRAP⁺ cells was decreased when compared with the group of 14-day ligation ($P < 0.01$).

Detection of the predominant immune-related leucocytes in different tissues

Flow cytometric analysis was used to quantify the frequencies of T and B cells in the cervical LN, spleen, and peripheral blood (Fig. 4). In the control group, CD3⁺ T cells and CD19⁺ B cells were the dominant population within the lymphocyte compartment among the cervical LN, spleen and peripheral blood (54.9% vs. 20.6%, 38.8% vs. 43.4%, and 37.3% vs. 37.5%, respectively).

Compared to the control group, the periodontitis group had a significantly higher level of CD19⁺ B cells in the cervical LN ($26.28 \pm 5.92\%$ vs. $20.57 \pm 3.19\%$, $P < 0.05$), whereas there were no significant changes of that in the spleen ($43.87 \pm 3.14\%$ vs. $43.38 \pm 4.08\%$, $P > 0.05$) or among PBMC ($34.77 \pm 10.01\%$ vs. $37.54 \pm 7.92\%$, $P > 0.05$). The proportion of CD3⁺ T cells in the cervical LN was decreased in the periodontitis group when compared with the control group, but the difference was not statistically significant ($50.52 \pm 5.27\%$ vs. $54.93 \pm 4.33\%$, $P > 0.05$). Likely, there were no significant differences of the frequencies of CD3⁺ T cells between the periodontitis group

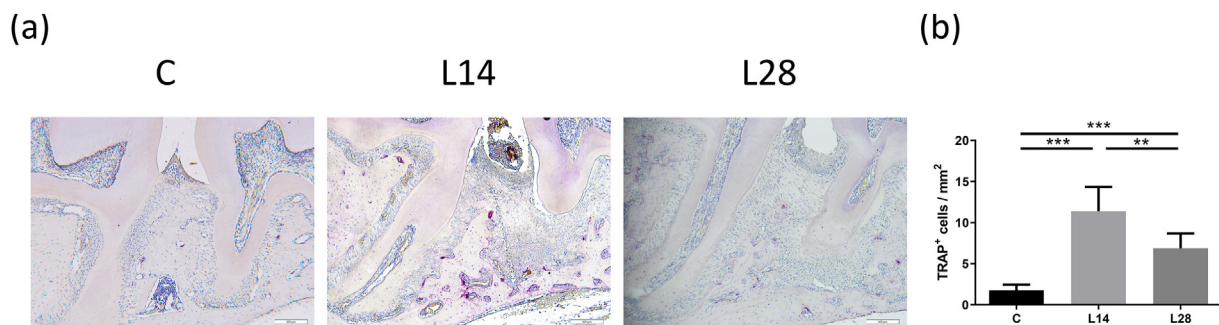


Fig. 3 Tartrate-resistant acid phosphatase staining. a) Representative images of the multinucleated osteoclasts in the different groups. The groups' names are abbreviated as follows: the control group (C), 14-day ligation group (L14), and 28-day ligation group (L28). Scale bars: 200 μm . b) Quantification analysis of the number of osteoclasts in the different groups. ** $P < 0.01$, *** $P < 0.001$.

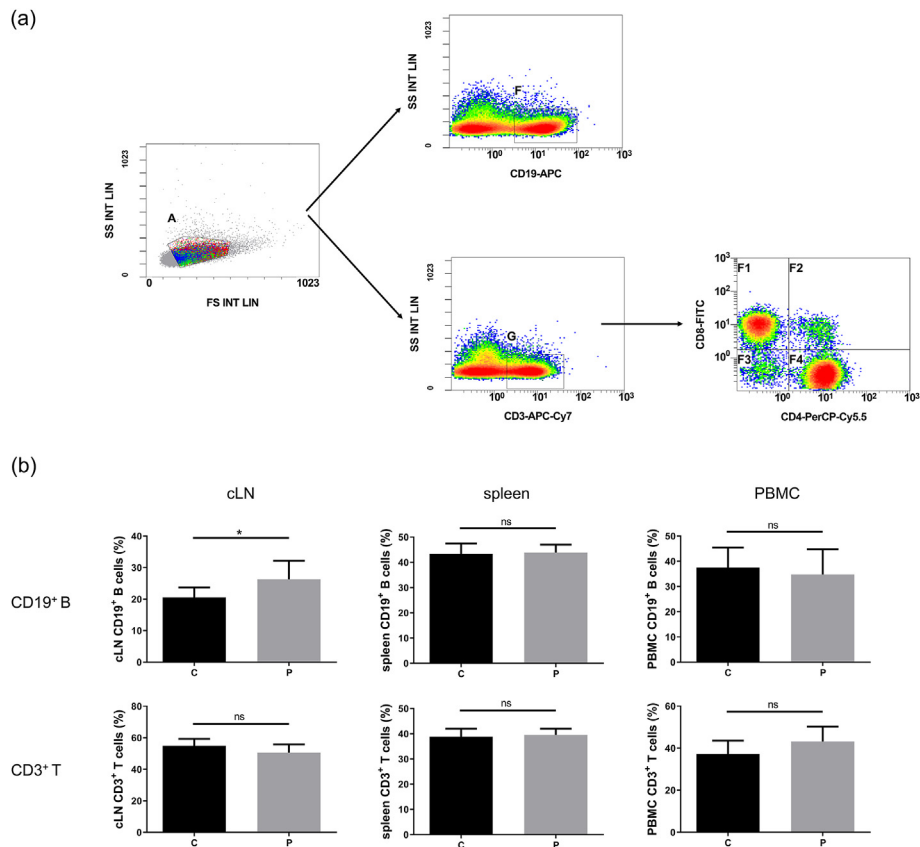


Fig. 4 Flow cytometric analysis of the predominant immune-related leucocytes. a) Gating strategies for flow cytometric analysis. B cells (CD19⁺), T cells (CD3⁺), CD4⁺ T cells (CD4⁺CD3⁺), CD8⁺ T cells (CD8⁺CD3⁺). b) The frequencies of CD19⁺ B cells and CD3⁺ T cells within different tissues. cLN: cervical lymph node, PBMC: peripheral blood mononuclear cell, C: the control group, P: the periodontitis group. * $P < 0.05$.

and the control group in the spleen ($39.51 \pm 2.44\%$ vs. $38.82 \pm 3.14\%$, $P > 0.05$) and PBMC ($43.14 \pm 7.08\%$ vs. $37.26 \pm 6.31\%$, $P > 0.05$).

In addition, the proportions of CD4⁺ T cells and CD8⁺ T cells among total CD3⁺ T cells in different tissues were further analyzed (Table 1). Although the proportions of CD4⁺ T cells in CD3⁺ T cell subset in all three types of tissues were elevated in the periodontitis group compared to the control group, the differences were not statistically significant ($P > 0.05$). Similarly, the frequencies of CD8⁺ T cells among total CD3⁺ T cells in the periodontitis mice were decreased in all three types of tissues, but all the differences were not statistically significant ($P > 0.05$). The changes resulted in a higher CD4⁺/CD8⁺ T cell ratio in all three types of tissues under periodontitis condition, yet, not statistically significant ($P > 0.05$).

Discussion

In the past few decades, a variety of animal models have been established to evaluate periodontal pathogenesis, several methods were used, such as ligature,¹⁵ injection of inactivated bacteria or bacterial lipopolysaccharide,¹⁶ oral gavage,¹⁷ and ligature soaked in bacteria.¹⁸ Because of the technical difficulty, the ligature-induced periodontitis model was not widely used until the first publish of detailed

description and images of the method.¹² Oral gavage and local injection methods are also used commonly, however, both of these methods generally take a longer time to

Table 1 Comparisons of the proportion of CD4⁺ T cells, the proportion of CD8⁺ T cells, and CD4⁺/CD8⁺ T cell ratio within different tissues between the control and periodontitis group.

Item	Tissue	Control group	Periodontitis group	P^c
CD4 ⁺ T cells in CD3 ⁺ T cells (%)	cLN ^a	62.64 ± 2.77	62.69 ± 2.36	0.970
	spleen	49.59 ± 6.52	53.14 ± 4.16	0.216
	PBMC ^b	60.71 ± 1.32	62.09 ± 3.18	0.311
CD8 ⁺ T cells in CD3 ⁺ T cells (%)	cLN ^a	31.51 ± 1.77	30.27 ± 1.09	0.115
	spleen	36.90 ± 4.09	34.11 ± 4.72	0.227
	PBMC ^b	31.22 ± 1.69	29.17 ± 2.84	0.127
The ratio of CD4 ⁺ T cells/CD8 ⁺ T cells in CD3 ⁺ T cells	cLN ^a	1.99 ± 0.19	2.08 ± 0.14	0.366
	spleen	1.37 ± 0.30	1.59 ± 0.27	0.150
	PBMC ^b	1.95 ± 0.12	2.14 ± 0.21	0.056

^a Cervical lymph node.

^b Peripheral blood mononuclear cell.

^c Independent two-tailed Student t tests.

produce significant periodontal tissues destruction than ligation.^{19,20} In addition, the severity of these two methods was inconsistent with different bacteria strains, concentrations of microorganisms, and mice background,^{21,22} while the principle of ligation model is based on the adherence of microorganisms around the ligature, initiating periodontitis through the colonization of bacteria.^{9,16} Considering the effectiveness and predictability, the ligature-induced mice model has become suitable, prevalent, and sufficiently established for periodontitis study.²³

The elicitation of significant bone loss is a major feature of experimental periodontitis model, our results of micro-CT scanning and H&E staining revealed that ligation could effectively induce significant periodontal inflammation and alveolar bone loss in C57BL/6J mice, which were maintained for a relatively long-term period. Further analysis of osteoclast counts by TRAP staining indicated that alveolar bone loss in the ligation model was progressive, characterizing as two different phases, with the occurrence of significant and rapid bone loss in the initial period, followed by continued progression in a relatively slow mode. Such findings were consistent with the previous studies.^{24–26} It is worth noting that the ligature-induced bone loss in the mouse model healed without any treatment after the ligature was removed.⁸ Based on the characteristic of this model and the results of our study, the healing potential of late-stage periodontitis could be studied with or without ligature removal.²⁷ Besides, when using the ligature-induced periodontitis model to study the effects of agents, the timing of drug administration should be determined more specifically and the results should be interpreted more cautiously. For instance, to assess the preventive effect, cytokines or molecules were inoculated before or at the same time of periodontitis induction.^{28,29} When the focus is on the treatment effect, intervention was carried out after the establishment of experimental periodontitis.^{30,31}

With the revelation of the theory called osteoimmunology, scholars are increasingly aware of the importance of the host immune response.³² Originally, T cells were the focus of research, the whole spectrum of cells mediating immunity such as B cells, macrophages, and neutrophils has become increasingly emphasized and investigated recently.³³ In the present study, samples for flow cytometric analysis were taken from the group of 14-day ligation, in which periodontitis was successfully established. Paralleling clinical observations of periodontal disease,⁷ our results showed that CD3⁺ T cells (50%–55%) and CD19⁺ B cells (21%–26%) were the dominant population within the lymphocyte compartment in the cervical LN that drain periodontal lesions in both health and disease condition. In addition, when compared to the healthy control, B cell population increased significantly in the periodontitis mice, while, although the proportion of T cell was much greater, there was no statistically significant change of T cell population. A recent study which used a novel CIBERSORT technology to profile human immune cell subtypes of healthy and periodontitis tissues also found that the plasma and naive B cells were elevated in periodontitis tissues.³⁴ As we aimed to investigate the change of immune-related cell population both locally and systemically, spleen and peripheral blood samples were also analyzed besides the cervical LN. However, neither B nor T

cell population in the spleen and peripheral blood showed a statistically obvious change in the periodontitis group compared to the control group. We hypothesized that the placement of a ligature leads to the imbalance of the periodontal ecosystem, altering the local immune micro-environment rather than the systemic immunoinflammatory state. A study in support of this hypothesis proposed that in experimental periodontitis, local stimulation alone may be insufficient to drive systemic inflammation and epigenetic modifications but could lead to epigenetic and inflammatory events following systemic microbial challenge.³⁵ Furthermore, the CD4⁺/CD8⁺ ratios were analyzed. Thus far, there has not been a consensus on the nature of CD4⁺/CD8⁺ ratios in periodontal disease lesions and peripheral blood.^{36,37} In our study, although the ratios showed an increasing trend at local and systemic level, the differences were not statistically significant, further investigations about this subject are required to determine the immunoregulation mechanisms effective in periodontal disease. Besides, genetically engineered or humanized immunodeficient mice were needed to study immunity-mediated pathology *in vivo*.^{9,38}

In conclusion, we performed the morphological, histological and cellular analysis in the ligature-induced periodontitis model in mice, which could provide important insights into the mechanisms of disease pathogenesis and progression. Moreover, based on the knowledge, more targeted strategies and new therapeutic modalities could be developed by acting at specific times in the development of periodontal disease or by targeting specific cell populations in the pathogenesis of periodontal disease.

Declaration of competing interest

The authors have no conflicts of interest relevant to this article.

Acknowledgements

This study was supported by grants from National Natural Science Foundation of China (No. 81470740, 81991500 and 81991502).

References

1. Kinane DF, Stathopoulou PG, Papapanou PN. Periodontal diseases. *Nat Rev Dis Prim* 2017;3:17038.
2. Slots J. Periodontitis: facts, fallacies and the future. *Periodontol* 2000 2017;75:7–23.
3. Lamont RJ, Koo H, Hajishengallis G. The oral microbiota: dynamic communities and host interactions. *Nat Rev Microbiol* 2018;16:745–59.
4. Ebersole JL, Dawson 3rd D, Emecen-Huja P, et al. The periodontal war: microbes and immunity. *Periodontol* 2000 2017; 75:52–115.
5. Han X, Kawai T, Taubman MA. Interference with immune-cell-mediated bone resorption in periodontal disease. *Periodontol* 2000 2007;45:76–94.
6. Kawai T, Matsuyama T, Hosokawa Y, et al. B and T lymphocytes are the primary sources of RANKL in the bone resorptive lesion of periodontal disease. *Am J Pathol* 2006;169:987–98.

7. Dutzan N, Konkel JE, Greenwell-Wild T, Moutsopoulos NM. Characterization of the human immune cell network at the gingival barrier. *Mucosal Immunol* 2016;9:1163–72.
8. Lin P, Niimi H, Ohsugi Y, et al. Application of ligature-induced periodontitis in mice to explore the molecular mechanism of periodontal disease. *Int J Mol Sci* 2021;22:8900.
9. Graves DT, Fine D, Teng YT, Van Dyke TE, Hajishengallis G. The use of rodent models to investigate host-bacteria interactions related to periodontal diseases. *J Clin Periodontol* 2008;35:89–105.
10. Gonzales JR. T- and B-cell subsets in periodontitis. *Periodontol* 2000 2015;69:181–200.
11. Percie du Sert N, Hurst V, Ahluwalia A, et al. The ARRIVE guidelines 2.0: updated guidelines for reporting animal research. *PLoS Biol* 2020;18:e3000410.
12. Abe T, Hajishengallis G. Optimization of the ligature-induced periodontitis model in mice. *J Immunol Methods* 2013;394:49–54.
13. Kızıldağ A, Arabacı T, Albayrak M, et al. Therapeutic effects of caffeic acid phenethyl ester on alveolar bone loss in rats with endotoxin-induced periodontitis. *J Dent Sci* 2019;14:339–45.
14. Hiyari S, Wong RL, Yaghsejian A, et al. Ligature-induced peri-implantitis and periodontitis in mice. *J Clin Periodontol* 2018;45:89–99.
15. Rovin S, Costich ER, Gordon HA. The influence of bacteria and irritation in the initiation of periodontal disease in germfree and conventional rats. *J Periodontol Res* 1966;1:193–204.
16. Klausen B. Microbiological and immunological aspects of experimental periodontal disease in rats: a review article. *J Periodontol* 1991;62:59–73.
17. Fiehn NE, Klausen B, Evans RT. Periodontal bone loss in Porphyromonas gingivalis-infected specific pathogen-free rats after preinoculation with endogenous Streptococcus sanguis. *J Periodontol Res* 1992;27:609–14.
18. Kimura S, Nagai A, Onitsuka T, et al. Induction of experimental periodontitis in mice with Porphyromonas gingivalis-adhered ligatures. *J Periodontol* 2000;71:1167–73.
19. Acqua YD, Hernández C, Fogacci M, Barbirato D, Palioto D. Local and systemic effects produced in different models of experimental periodontitis in mice: a systematic review. *Arch Oral Biol* 2022;143:105528.
20. de Molon RS, de Avila ED, Cirelli JA. Host responses induced by different animal models of periodontal disease: a literature review. *J Investig Clin Dent* 2013;4:211–8.
21. de Molon RS, de Avila ED, Boas Nogueira AV, et al. Evaluation of the host response in various models of induced periodontal disease in mice. *J Periodontol* 2014;85:465–77.
22. de Molon RS, Mascarenhas VI, de Avila ED, et al. Long-term evaluation of oral gavage with periodontopathogens or ligature induction of experimental periodontal disease in mice. *Clin Oral Invest* 2016;20:1203–16.
23. Marchesan J, Girnary MS, Jing L, et al. An experimental murine model to study periodontitis. *Nat Protoc* 2018;13:2247–67.
24. de Molon RS, Park CH, Jin Q, Sugai J, Cirelli JA. Characterization of ligature-induced experimental periodontitis. *Microsc Res Tech* 2018;81:1412–21.
25. Wu YH, Taya Y, Kuraji R, Ito H, Soeno Y, Numabe Y. Dynamic microstructural changes in alveolar bone in ligature-induced experimental periodontitis. *Odontology* 2020;108:339–49.
26. Vargas-Sanchez PK, Moro MG, Santos FAD, et al. Agreement, correlation, and kinetics of the alveolar bone-loss measurement methodologies in a ligature-induced periodontitis animal model. *J Appl Oral Sci* 2017;25:490–7.
27. Wong RL, Hiyari S, Yaghsejian A, et al. Comparing the healing potential of late-stage periodontitis and peri-implantitis. *J Oral Implantol* 2017;43:437–45.
28. Greene AC, Shehabeldin M, Gao J, et al. Local induction of regulatory T cells prevents inflammatory bone loss in ligature-induced experimental periodontitis in mice. *Sci Rep* 2022;12:5032.
29. Cafferata EA, Terraza-Aguirre C, Barrera R, et al. Interleukin-35 inhibits alveolar bone resorption by modulating the Th17/Treg imbalance during periodontitis. *J Clin Periodontol* 2020;47:676–88.
30. Wang J, Wang B, Lv X, Wang L. NIK inhibitor impairs chronic periodontitis via suppressing non-canonical NF- κ B and osteoclastogenesis. *Pathog Dis* 2020;78. ftaa045.
31. Lee J, Min HK, Park CY, Kang HK, Jung SY, Min BM. A vitronectin-derived peptide prevents and restores alveolar bone loss by modulating bone re-modelling and expression of RANKL and IL-17A. *J Clin Periodontol* 2022;49:799–813.
32. Graves DT, Li J, Cochran DL. Inflammation and uncoupling as mechanisms of periodontal bone loss. *J Dent Res* 2011;90:143–53.
33. Gruber R. Osteoimmunology: inflammatory osteolysis and regeneration of the alveolar bone. *J Clin Periodontol* 2019;46:52–69.
34. Li W, Zhang Z, Wang ZM. Differential immune cell infiltrations between healthy periodontal and chronic periodontitis tissues. *BMC Oral Health* 2020;20:293.
35. Palioto DB, Finoti LS, Kinane DF, Benakanakere M. Epigenetic and inflammatory events in experimental periodontitis following systemic microbial challenge. *J Clin Periodontol* 2019;46:819–29.
36. Erciyas K, Orbak R, Kavrut F, Demir T, Kaya H. The changes in T lymphocyte subsets following periodontal treatment in patients with chronic periodontitis. *J Periodontol Res* 2006;41:165–70.
37. Demir T, Canakci V, Erdem F, Atasever M, Kara C, Canakci CF. The effects of age and gender on gingival tissue and peripheral blood T-lymphocyte subsets: a study in mice. *Immunol Invest* 2008;37:171–82.
38. Rojas C, Garcia MP, Polanco AF, et al. Humanized mouse models for the study of periodontitis: an opportunity to elucidate unresolved aspects of its immunopathogenesis and analyze new immunotherapeutic strategies. *Front Immunol* 2021;12:663328.